JCI The Journal of Clinical Investigation

Zika virus infects human testicular tissue and germ cells

Giulia Matusali, … , Anna Le Tortorec, Nathalie Dejucq-Rainsford

J Clin Invest. 2018. https://doi.org/10.1172/JCI121735.

Research In-Press Preview **Virology**

Zika virus (ZIKV) is a teratogenic mosquito-borne flavivirus which can be sexually transmitted from man to woman. High viral loads and prolonged viral shedding in semen suggest that ZIKV replicates within the human male genital tract, but its target organs are unknown. Using ex vivo infection of organotypic cultures, we demonstrated here that ZIKV replicates in human testicular tissue and infects a broad range of cell types, including germ cells, which we also identified as infected in the semen from ZIKV-infected donors. ZIKV had no major deleterious effect on the morphology and hormonal production of the human testis explants. Infection induced a broad antiviral response but no interferon up-regulation and minimal pro-inflammatory response in testis explants, with no cytopathic effect. Finally, we studied ZIKV infection in mouse testis, and compared it to human infection. This study provides key insights into how ZIKV may persist in semen and alter semen parameters, as well as a valuable tool for testing antiviral agents.

Zika virus infects human testicular tissue and germ cells

Giulia Matusali[1], Laurent Houzet[1], Anne-Pascale Satie[1], Dominique Mahé[1], Florence Aubry[1], Thérèse Couderc[2,3], Julie Frouard[1], Salomé Bourgeau[1], Karim Bensalah[4], Sylvain Lavoué[5], Guillaume Joguet[6], Louis Bujan[7], André Cabié[8], Gleide Avelar[9], Marc Lecuit[2,3,10], Anna Le Tortorec[1], Nathalie Dejucq-Rainsford[1]*

[1] *Univ Rennes, Inserm, EHESP, Irset (Institut de recherche en santé, environnement et travail) - UMR_S1085, F-35000 Rennes, France*
[2] *Institut Pasteur, Biology of Infection Unit, Paris, France*
[3] *Inserm U1117, Paris, France*
[4] *Service d'Urologie, Centre Hospitalier Universitaire de Rennes, F-35000 Rennes, France*
[5] *Unité de coordination hospitalière des prélèvements d'organes et de tissus, Centre Hospitalier Universitaire de Rennes, F-35000 Rennes, France*
[6] *Centre Caribéen de Médecine de la Reproduction-CECOS CHU de Pointe à Pitre Guadeloupe, France*
[7] *Research Group on Human Fertility EA 3694, University Paul Sabatier Toulouse III-CECOS, Hôpital Paule de Viguier, CHU Toulouse, Toulouse, France*
[8] *Inserm Centre d'Investigation Clinique 1424, Centre Hospitalier Universitaire de Martinique, France; Service de maladies infectieuses, Centre Hospitalier Universitaire de Martinique, France*
[9] *Department of morphology, Federal University of Minas Gerais, Belo Horizonte, Brazil*
[10] *Paris-Descartes University, Department of Infectious Diseases and Tropical Medicine, Necker-Enfants Malades University Hospital, Paris, France*

*Corresponding author:
Nathalie DEJUCQ-RAINSFORD
IRSET-Inserm U1085
9 avenue du Pr Léon Bernard
F-35000 Rennes, France
E-mail : nathalie.dejucq-rainsford@univ-rennes1.fr
Phone : +33 2 2323 5069

The authors declare no conflict of interest.

Word count: 10686

ABSTRACT

Zika virus (ZIKV) is a teratogenic mosquito-borne flavivirus which can be sexually transmitted from man to woman. High viral loads and prolonged viral shedding in semen suggest that ZIKV replicates within the human male genital tract, but its target organs are unknown. Using ex vivo infection of organotypic cultures, we demonstrated here that ZIKV replicates in human testicular tissue and infects a broad range of cell types, including germ cells, which we also identified as infected in the semen from ZIKV-infected donors. ZIKV had no major deleterious effect on the morphology and hormonal production of the human testis explants. Infection induced a broad antiviral response but no interferon up-regulation and minimal pro-inflammatory response in testis explants, with no cytopathic effect. Finally, we studied ZIKV infection in mouse testis, and compared it to human infection. This study provides key insights into how ZIKV may persist in semen and alter semen parameters, as well as a valuable tool for testing antiviral agents.

Keywords: Zika virus; sexual transmission; semen; human testis; organotypic culture; tropism; germ cells; macrophages; Sertoli cells; peritubular cells; Leydig cells; innate immune response; interferons; inflammation; mouse testis.

INTRODUCTION

Zika virus (ZIKV) is a teratogenic arthropod-borne flavivirus, which recently emerged in the Pacific (2007), Oceania (2013) and the Americas (2015).

While ZIKV's primary mode of transmission is through mosquito bites, male-to-female sexual transmission has been reported by cohort studies (1, 2), and by case reports in non-endemic countries (3). Importantly, male-to-female sexual transmission in animal models was found to enhance viral dissemination in the female genital tract and transmission to the fetus (4–8). In humans, high viral loads and prolonged shedding of viral RNA (vRNA) and infectious virus (up to 1 year and 69 days, respectively) in the absence of viremia have been found in semen (9–11), strongly suggesting a tropism of ZIKV for the male genital tract. Studies in immunodeficient mice evidenced high levels of ZIKV infection within the testis, leading to orchitis and impaired testosterone and sperm production (12–15). However, these mouse models do not reflect the pathophysiology in humans: unlike humans, mice only become infected following abrogation of type I interferon (IFN) signaling and die of infection in most cases. This defective antiviral response may enhance the susceptibility and pathogenicity of ZIKV. In sharp contrast, ZIKV infection in macaque models either spared the testis or led to a moderate infection, with no deleterious effects observed (16–18). Interestingly, a recent study on 15 ZIKV-infected men reported a lower total sperm count at day 30 post symptoms onset compared with day 7, suggesting an effect of the infection on the testis or epididymis (19).

Here, by infecting with ZIKV testicular tissue explants from healthy donors, we show that ZIKV replicates and produces infectious viral particles in human testis. We evidence infection of a broad range of testicular cell types, including resident macrophages and the germ cell line, and confirm the latter in patients' semen. Infection had no effect on basal testosterone and inhibin B production or overall cell viability ex vivo. ZIKV triggered a wide range of antiviral genes in human testes, but up-regulation of types I, II and III IFN was not observed and pro-inflammatory

response was minimal. Finally, our data on IFNAR-/- mice points at similarities and differences between mouse and human testis to ZIKV infection.

RESULTS

ZIKV replicates in human testicular tissue

Testis explants from 8 uninfected donors were exposed to ZIKV ex vivo and maintained in culture medium as previously described (20). We first assessed the replication rate of a ZIKV strain derived from the 2015 outbreak in the Americas, by measuring viral release over 3-day-culture periods at day 3, day 6 and day 9 post-infection (p.i.). A significant increase in the levels of vRNA release rate was observed between days 3-6 (median 5.85 x 10^7 copies/ml) and 6-9 (median 8.28 x 10^7 copies/ml) compared to days 0-3 p.i. (median 5.29 x 10^6 copies/ml) (Figure 1A), while vRNA was below the detection threshold in mock-infected testes (not shown).

Testis ability to produce infectious ZIKV particles was tested on reporter VeroE6 cells. A significant increase in supernatants infectivity was observed between days 0-3 (median 3 x 10^2 $TCID_{50}$/ml) and days 6-9 p.i. (median 7.50 x 10^4 $TCID_{50}$/ml), demonstrating the infectivity of viral progeny (Figure 1B). The highest cumulative titer at day 9 (i.e. reflecting infectious viral production throughout culture) was 2 x 10^6 $TCID_{50}$/ml (Figure S1), with a median of 3.16 x 10^5 $TCID_{50}$/ml. Similarly, vRNA and infectious virion release rates increased during the culture of testis explants exposed to another ZIKV strain isolated during the 2013 outbreak in French Polynesia (Figure S2).

Altogether, these data demonstrate that ZIKV efficiently infects and replicates in the human testis ex vivo, producing infectious viral particles.

ZIKV infects somatic and germ cells in human testis explants

To determine ZIKV's the target cells in the human testis, mock or ZIKV-infected testis explants were submitted to RNAscope in situ hybridization (ISH) using probes specific for ZIKV RNA (Figure 2A-H, controls in Figures 2A and S3), and to immunohistochemistry using an antibody against the non-structural NS1 viral protein (Figure 2I-M)Figure FigureFigure. Infected testes

displayed strong vRNA staining of the interstitial tissue cells and within the extracellular matrix bordering the seminiferous tubules, along with a more diffuse staining in some interstitial areas (Figure 2B-F). A weaker dotty staining was also observed inside a few seminiferous tubules (Figure 2G-H), suggestive of association of the ZIKV with germ cells (Figure 2G) and Sertoli cells (Figure 2H). NS1 antibody (Figure 2I-M) similarly labeled cells within the seminiferous tubule wall (Figure 2I) and the interstitium (Figure 2J), demonstrating ZIKV replication in these target cells. Within the tubules, different germ cell categories including spermatogonia (identified based on their position in the seminiferous epithelium, nucleus size and distinctive morphological features) (Figure 2K) and a few Sertoli cells (identified based on distinctive nucleus shape) (Figure 2L), stained positive for NS1. Infected cells (vRNA+ or NS1+) displayed similar localization at the different time points of infection (days 3, 6 and 9) for the two ZIKV strains tested (Figure S4 and data not shown).

To further identify the nature of the infected cells, we combined ISH for vRNA with fluorescent immuno-labelling for specific cell markers, and undertook quantification of infected cells in testicular tissue from 4 donors. Interstitial infected cells were primarily CD68/CD163+ testicular macrophages (median 12.7 cells/mm^2), and to a lesser extent CYP11A1+ Leydig cells (median 3 cells/mm^2) (Figure 3A, B, G). Staining for α smooth actin (αSMA) demonstrated the infection of myoid peritubular cells bordering the seminiferous tubules (median 10 cells/mm^2) (Figure 3C, G). Within the tubules, dotty fluorescent ZIKV staining close to the lumen histologically co-localized with late germ cells (Figure 3D). Such staining was also present at the base of the tubules, where co-labeled DDX4+ early germ cells were evidenced (DDX4 being a specific marker expressed by most of the germ cells) (Figure 3E). Staining was never observed when using a vRNA probe on mock-infected negative controls (Figure 3F). Infected cells in seminiferous tubules were mostly germ cells (median 11 cells/mm^2), while infected Sertoli cells represented a median of 3.5 cells/mm^2 (Figure 3G).

Collectively these data indicate that ZIKV has a tropism for germ cells and somatic cells within the human testis.

ZIKV replicates in human testicular germ cells in vitro and in vivo

We exposed freshly-isolated seminiferous tubules cells o ZIKV to investigate their ability to produce infectious viral particles which might be released into semen. In 3 independent primary cultures, vRNA increased in cells from a median of 2.82 x 10^3 to 2.09 x 10^7 copies/µg total RNA between 6h and 120h p.i. (Figure 4A). ZIKV RNA in culture supernatants significantly increased of about 4 log10 between 6h and 120h p.i. (median values of 1.26 x 10^4 and 5.01 x 10^7 copies/ml respectively) (Figure 4B). Infectious virus titers also rose between 48h and 120h, reaching a median of 4 x 10^5 $TCID_{50}$/ml and maximum titer of 4 x 10^6 $TCID_{50}$/ml (Figure 4C). ZIKV replicated in DDX4+ germ cells, FSH receptor+ Sertoli cells and αSMA+ peritubular cells (Figure 4D). ZIKV envelope (ZIKV-E) was detected in undifferentiated spermatogonia (MAGEA4+ Stra8-) and in MAGEA4+ Stra8+ cells, corresponding to differentiated spermatogonia up to preleptotene spermatocytes stage (Figure 4D).

To further explore the germ cells' productive infection and since primary testicular germ cells cannot be cultured without somatic support, we used the seminoma-derived germ cell line T-cam2, which displays characteristics of fetal germ cells (21). In 3 independent experiments, vRNA in T-cam2 cells rose from below detection at 6h to a median of 6.31 x 10^5 copies/µg total RNA at 72h p.i., reaching up to 1 x 10^6 copies/ml in culture supernatants (Figure S5A, B). ZIKV-E was evidenced in T-cam2 by immunofluorescence (Figure S5C). The production of infectious viral particles was evidenced in the two cultures showing the highest viral loads, with a maximum titer of 8.2 x 10^3 $TCID_{50}$/ml (Figure S5D).

These findings were corroborated in vivo by analyzing the semen cell smear from two ZIKV-infected donors, in which we revealed the presence of ZIKV-E or NS1+ germ cells exfoliated from

the testis 7 days and 11 days post-symptoms onset (Figure 4E). A subset of spermatozoa also labelled for ZIKV-E (Figure S6).

Altogether, these data indicate that ZIKV replicates in human germ cells at different stages of differentiation and infects testicular germ cells in ZIKV-infected men.

ZIKV infection ex vivo has no major impact on human testis morphology or hormonal production

We next assessed the impact of ZIKV on human testis morphology, viability and function during the ex vivo culture time frame. The tissue architecture and histology of infected testes were similar to that of mock-infected testes all throughout the culture period (Figure 5). In both infected and mock-infected testes we observed conserved interstitial tissue (comprising groups of Leydig cells, mast cells, and blood vessels), seminiferous basement membrane of similar thickness (increased thickness being a sign of injury), and seminiferous tubules encompassing Sertoli cells and early and late germ cells (Figure 5 A, D). Caspase-dependent apoptosis evidenced by cleaved caspase 3 immunostaining was similar in infected and mock-infected testis and, as expected, primarily affected isolated germ cells (Figure 5B). The measurement of LDH release confirmed that the overall viability of the organ was not affected by the infection (Figure 5C). Testosterone concentrations were not different in infected versus mock-infected testes (Figure 5E), and the expression of genes encoding steroidogenic enzymes unmodified by ZIKV (Figure S7 A). Sertoli cells positively stained for the tight junction marker protein ZO-1 in both infected and mock-infected testis until day 9 p.i., suggesting an intact barrier (Figure 5 F). Inhibin B (a marker of Sertoli cell function) protein and mRNA levels showed no significant differences between infected and mock-infected testis up to day 9 p.i. (Figure 5G and Figure S7 B). Finally, the levels of peritubular cells (Acta2), early meiotic (PGK2) and late post-meiotic (PRM2) germ cells transcripts were unchanged by the infection (Figure S7 B).

Overall, although actively replicating within the testis, ZIKV did not appear to affect testis morphology, induce cell death, or trigger any drastic effect on the testis functions during the 9-day culture.

ZIKV triggers a broad antiviral response but no IFN-up-regulation and a minimal pro-inflammatory response in human testicular tissue

To investigate the immune response to ZIKV infection, we assessed the concentration of a panel of antiviral and pro-inflammatory cytokines (IFNβ, IFNα2, IFN λ1, IFN λ2/3, IFNγ, IL1β, IL6, TNFα, IL8, IL-12p70, CXCL10, IL-10 and GM-CSF) in testis explant supernatants. Type I, II and III IFN concentrations in testis culture supernatants were unchanged by the infection at days 3 and 6 p.i. in 7 independent testis cultures tested (Figure 6A and S8). Among pro-inflammatory cytokines, only CXCL10 was significantly increased (Figure 6A and S8), and its induction positively correlated with vRNA load (Figure 6B).

We then analysed the transcripts of 11 of these cytokines (IFNβ, IFNα1, IFNα2, IFNα4, IFNλ1, IFNλ2, IFNλ3, IL-1β, IL-6, TNFα, and CXCL10) by RT-qPCR on ZIKV-infected versus mock-infected testes. Type I, II and III IFN transcripts in uninfected testis tissues were below the measurement threshold irrespective of infection (data not shown), while CXCL10 was increased (median fold change (FC) 43.4 at day 9, range 7.7-227.8) in the testis from 4 out of 6 donors (Figure 6C).

Extending the analysis to a wider range of genes involved in pathogen sensing (RIG-I, MDA5), antiviral response (IFNε, IFI27, IFIT1, IFITM1, IRF7, ISG15, Mx1, Mx2, OAS1, OAS2, RSAD2), inflammation (CCR7, CD14, CD64, HLA-DR, MCSF), chemoattraction (CCL2, CCL5, CXCL1, CXCL2,), and control of inflammation (IL-10, TGFβ, CD163, SOCS1, SOCS3), we observed the induction of a broad range of antiviral genes from day 3 onwards in the testis from 3 out of 6 donors and at day 9 in one other donor (Figure 6C).

A strong induction of ISG15 (FC 12.2, range 5.2-45.6), IFIT-1 (FC 12.8, range 9.7-29.6), OAS1 (FC 22.9, range 6.4-32.5), OAS2 (FC 7.1, range 4.2-21.6), Mx1 (FC 9.8, range 5.1-35.1), Mx2 (FC 9.5, range 3.7-25.3) and RSAD2 (FC 31.5, range 3.7-66.8) was measured at day 9 in these 4 donors, along with a relatively more moderate induction of IFI27 (FC 3.1, range 2.2-10.6), IFITM1 (FC 1.8, range 1.5-6.2), IRF7 (FC 2.7, range 1.8-6), MDA5 (FC 1.9, range 1.6-8.5) and RIG-1 (FC 2.8, range 1.8 to 9.4) (Figure 6C).

The fold change of these genes at day 9 correlated one to another, except for IFITM1 and MDA5 (Figure S9). The fold increase at day 9 of a number of genes involved in the antiviral response (RSAD2, IFIT1, ISG15, OAS1, OAS2, Mx1, Mx2, IFI27, IRF7), pathogen sensing (RIG1), and CXCL10 positively correlated with the level of infection (shown in Figure 6B) in the corresponding testis supernatant at days 3 and 6 (Figure 6E and Figure S9).

Finally, we assessed expression levels of all transcripts, including type I, II and III IFN, at earlier time points (4h, 18h, 48h p.i.) in two testis explants, and did not observe any up-regulation (Figure S10 and data not shown).

Altogether, these results are consistent with ZIKV infection inducing a broad antiviral and minimal pro-inflammatory response in the absence of detectable IFN stimulation in human testis explants.

Innate immune response to ZIKV infection in the testis from IFNAR$^{-/-}$ mouse

To support our hypothesis of a type I IFN independent antiviral response induced by ZIKV in testis and compare our findings on ZIKV tropism and initial antiviral/pro-inflammatory responses in human testis explants versus that in a widely-used animal model, we analysed the testis of type I IFN receptor-defective (IFNAR$^{-/-}$) mice using similar techniques and viral strain.

ZIKV RNA measurement in testes from IFNAR$^{-/-}$ mice infected for 5 and 9 days showed high viral loads in this organ (Figure 7A). Despite differences in intensity and sequence of infection, ZIKV tropism in the mouse testis in vivo was comparable overall to that in human testis ex vivo. At day 5,

testicular infection localized primarily within the interstitial tissue and the peritubular cells, while seminiferous tubules were spared (Figure 7B). Co-labeling of ZIKV RNA with cell markers showed infection of STAR+Leydig cells and F4/80+ macrophages (Figure 7C). At day 9 p.i. (a time at which some mice started to die), strong labeling for vRNA became prominent within Sertoli and germ cells (Figure 7B). We did not observe modifications of testicular morphology at these early time points, in agreement with previous studies (12, 22).

We next examined the induction of genes involved in antiviral response and inflammation in mouse testis (Figure 7D). Similar to human testis explants, and despite a lack of type I IFN signaling, a strong induction of ISG15 (FC 11.7, range 7.7-15.6 at day 5 and FC 7.4, range 4.7-15.1 at day 9), RSAD2 (FC 24.6, range 13.7-45.6 at day 5, and FC 10.1, range 2.21-30.39 at day 9), IFIT1 (FC 36.0, range 19.5-42.6 at day 5, and FC 10.1, range 6.2-27.3 at day 9) and CXCL10 (FC 17.5, range 9.4-39.2 at day 5, and FC 9.0, range 4.2-14.6 at day 9) was measured in infected mice testis (Figure 7D). In contrast to human testis, Mx1, MDA5 and RIG-1 were not induced at either day 5 or day 9 (Figure 7D). These results suggest that ZIKV induces a type I IFN signaling-independent antiviral response in both humans and mice. In contrast to human testis, in which CXCL10 was the only pro-inflammatory gene increased by the infection, TNFα (median fold change 48.0, range 32.6-122.6 at day 5, and median 6.9, range 2.6-12.3 fold at day 9), IL-1β (median 7.7, range 1.8-13.8 fold at day 5 only) and IL-6 (median 10.7, range 4.9-27.5 fold at day 5 only) were up-regulated in infected mouse testis (Figure 7D), while IFNγ (produced by NK and T cells) was maximally increased at day 9 (median 11.2, range 6.2-30.8 fold) over day 5 (median 6.2, range 4.0-12.7 fold). IFNβ was the most dramatically-stimulated innate immune gene at day 5 (median 236.7, range 130.2-353.4 fold), while IFNα1, 2, 4 genes were modestly and transiently up-regulated at day 5 and IFNλ2/3 mRNAs levels were unchanged (Figure 7D). When looking at markers of immune cell subtypes, a transient increase in transcripts encoding the myeloid cell marker CD14 was observed at day 5, whereas transcripts encoding CD3 (T cell marker) and CD8 (cytotoxic T cell marker) were maximally up-

regulated at day 9, in line with the IFNγ expression pattern. The markers for B cells (CD19 and CD20), regulatory T cells (FoxP3) and macrophages (CD68) were unchanged, while CD4 (expressed by T helper and myeloid cells) was down-regulated (Figure 7D). The infiltration of T lymphocytes in infected mouse testis was confirmed by CD3 immunostaining and quantification of positive cells (Figure S11), further demonstrating mouse testis inflammation.Overall, the induction of an antiviral response in human and IFNAR$^{-/-}$ mice testis supports the existence of a type I IFN signaling independent response to ZIKV infection in testis.

DISCUSSION

We show that Asian ZIKV replicates in the human testis ex vivo. . Infected somatic cells within testis explants were mostly macrophages and peritubular cells, while a lower number of Leydig cells and Sertoli cells were observed. Considering the relative proportion of these different cell types in human testicular tissue (approximately one macrophage for 10 Leydig cells, 36 peritubular cells, 40 Sertoli cells and 400 germ cells) (23, 24), macrophages are likely the cell type most susceptible to ZIKV infection within the testis. Importantly, we demonstrate that ZIKV replicates within testicular germ cells, from stem cell (spermatogonia) to spermatozoa precursors (spermatids). In agreement, Robinson et al. lately reported on the infection of male germ cells after 3 days exposure of human seminiferous tubules to African ZIKV (25). Our detection of infected germ cells in semen from ZIVK-infected men confirms these in vitro and ex vivo findings.. The presence of ZIKV in ejaculated spermatozoa adds to previous findings of ZIKV antigen, RNA and infectious particles in spermatozoa (19) (26). Spermatozoa and immature germ cells may be infected during epididymal transit (duration 1 to 21 days) or within the testis. To infect these cells, the virus has to cross the blood testis barrier formed by the Sertoli cell tight junctions. Direct infection of the Sertoli cells is supported by our results in primary cells and that of other authors in commercial Sertoli cells (27, 28). Sertoli cells were showed to release ZIKV particles on their adluminal side, whereas the tight and adherens junction protein expression was not altered by infection (27). In agreement with these data, the ZO-1 labelling we observed in human explants suggested intact Sertoli cell barrier despite infection. In contrast, Sertoli cell exposure to inflammatory mediators produced by ZIKV-infected blood-derived macrophages (which phenotype differs from that of the anti-inflammatory testicular macrophages) altered their barrier function (27). Thus, the alteration of the blood-testis-barrier by testis-infiltrating macrophages may provide an additional way for the virus to reach seminal lumen and late germ cells. Altogether, our data show

290 that ZIKV replicates in germ cells and suggest that the virus might be able to bypass the blood testis
291 barrier by infecting Sertoli cells.

292 In our ex vivo model, testosterone and inhibin B release were not modified by infection, nor
293 were their related gene expression. This is not a limitation of our culture system since it is
294 successfully used to assess the hormonal production of human testis (29). This lack of effect might
295 be linked to low infection levels of Leydig and Sertoli cells ex vivo, as supported by relatively low
296 number of infected cells. In ZIKV-infected mouse testis, testosterone and inhibin B levels were
297 preserved at day 7 p.i. while testis integrity was still maintained, whereas they decreased after
298 orchitis (12, 13), suggesting that inflammation rather than testis infection caused altered hormone
299 secretion. In a 4-month follow-up of a cohort of 15 ZIKV-infected men, testosterone levels were not
300 significantly affected, whereas slightly lower inhibin B levels were reported at day 7 post-symptoms
301 onset compared with later time points (19). Such transient imbalance of reproductive hormones can
302 be related to fever or other systemic effects (30). However, we did not study the effect of ZIKV on
303 LH- and FSH-stimulated hormone secretion, and a systemic impact on testicular hormones in vivo
304 cannot be ruled out. Moreover, we cannot exclude effects at the single cell level that cannot be
305 detected when analyzing the whole tissue.

306 Our findings suggest that ZIKV could affect sperm production. Beside germ cell infection,
307 somatic cell infection might disrupt theparacrine control of spermatogenesis (31, 32), and the
308 infection of the contractile peritubular cell (33) might decrease the expulsion of spermatozoa from
309 tubules into the epididymis, . Infected men showed a decrease in sperm count and an increase in
310 spermatozoa abnormalities during the 2 months post clinical onset (19, 34). Our results suggest that
311 direct infection of germ and/or testicular somatic cells might be involved in such altered sperm
312 parameters, although fever and/or immune response could be involved (35, 36).

The infection had no significant effects on testis explants morphology nor viability. This is in contrast to findings in mouse models where damaging effects of ZIKV infection on testis became evident after leukocytes' infiltration (12–14). Since the ex vivo testis model lacks the presence of an intact immune system, we cannot rule out an effect of acquired immunity on the testis from ZIKV-infected men. However, testicular atrophy or orchitis have never been reported in clinical cases or non-human primate studies, and immune infiltrations were not observed in the latter (16–18), suggesting the absence of massive inflammation. The lack of cell death induction in our ex vivo model could be linked to culture conditions (e.g. viral strains/doses used, duration of infection) or to the limited number of infected cells. However, it might also reflect the ability of the virus to replicate in testicular cells in a non-cytopathic manner. Non or minimal cytopathic infection and persistence of ZIKV has been reported in different cell types, including human placental macrophages (37), brain microvascular endothelial cells (38), and lately, male mouse germ cells (25). Absence of cytopathic effect was also reported in Sertoli cells infected with ZIKV (27, 39). In contrast, high cytotoxicity was reported in ZIKV-infected human testis organoids (40). However, in this organoid system, the architecture of the testis is not preserved and physiological cellular interactions lost. Altogether, we hypothesize that non-lytic infection, in combination with evasion from immune responses, may allow viral persistence in the human testis.

. A broad range of antiviral genes was induced by ZIKV in testis explants. Several of these classically-defined Interferon-Stimulated Genes (ISGs), such as ISG15 (41), RSAD2 (42), IFITM1 (43), OAS1 (44), Mx1 (45) and IFIT gene family members (46) have an inhibiting activity on flaviviruses and/or ZIKV replication. Most interestingly, ZIKV did not increase type I, II or III IFNs secretion by testicular explants, and their transcripts consistently remained below detection at all time points. A level of IFN production below the sensitivity of our assays, or an active inhibition of IFN production by ZIKV, could explain these results. Thus, ZIKV non-structural proteins inhibit different steps of type I IFN induction cascade (47, 48). Alternatively, the absence of IFN up-

regulation in testis explants might reflect a specificity of this immune-suppressed organ, in which sustained high concentrations of type I IFN trigger germ cell apoptosis and sterility (49). Detection of ISGs over-expression in the testis from ZIKV-infected IFNAR-/- mice further suggest IFN-independent induction of ISGs in the testis. The increased level of RIG-1 mRNA in infected testis suggests it may be involved in the direct induction of ISGs, although other effectors could be in play (50). However, the broad induction of ISGs may fail to control ZIKV replication in the testis in the absence of increased type I IFN secretion to amplify and stabilize the antiviral response. In contrast to antiviral genes, ZIKV infection of the human testis did not affect any of the classic pro-inflammatory cytokines, except for CXCL10 which secretion was modestly increased. Interestingly, the level of antiviral transcripts at day 9 p.i. positively correlated with the level of infection at days 3 and 6, suggesting that the initial level of infection influenced the intensity of the antiviral response. Accordingly, antiviral genes were not induced in explants showing lower levels of infection. Thus host factors other than those we have studied may play a role in susceptibility to ZIKV. Altogether, our results indicate that ZIKV induces a broad induction of antiviral effectors but no IFN up-regulation and minimal pro-inflammatory response in ex vivo infected human testis. We hypothesize that such innate immune response, along with a lack of cytopathic effect, might facilitate the persistence of ZIKV for extended periods in the testis, and contribute to the prolonged release of ZIKV in semen.

Animal models are crucial for mechanistic studies and the in vivo testing of antiviral strategies. Cross-validation with human data is essential to assess their similarities and differences. Discrepant results on the interstitial (13, 22, 51) and/or intratubular localization of ZIKV (15, 17, 67, 68, 69) were reported in mouse testis from IFN-signaling deficient mice. Our results in the $IFNAR^{-/-}$ mouse model reconciled these results since ZIKV infection was exclusively located in interstitial cells and peritubular cells at day 5 p.i., whereas by day 9 the infection had progressed to the seminiferous tubules where it became prominent. In human testis, seminiferous tubule cell

infection was consistently weaker than that in the mouse and that in human interstitial cells.. This was not modified when increasing the infective viral dose 10 times (not shown). The difference in seminiferous tubule infection level in mice versus humans might reflect differences in the susceptibility of mouse-versus-human Sertoli and germ cells to ZIKV infection and/or in their innate immune response.

Like in human testis, we evidenced several ISG mRNA induction in the testis from IFNAR$^{-/-}$ mice, indicating a type I IFN-signaling independent induction that corroborates our results in human testis explants. Interestingly, in contrast to the human testis, the pathogen sensor RIG-1 was not up-regulated in the mouse testis, which may suggest different sensing mechanism. Unlike human testis also, type I IFNs and a number of pro-inflammatory genes were upregulated in mice. We previously showed that unlike their rodent counterparts, which produced large amounts of IFN, primary human Leydig cells did not produce IFN in response to paramyxovirus infection or double strand RNA stimulation (54, 55). This key difference between mouse and human testis in terms of IFN production may explain why in IFN-signaling competent mice, ZIKV tropism has been reported as essentially restricted to germ cells (25), whereas a broad tropism for both somatic and germ cells is observed in human testis explants and in IFNAR -/- mice. Indeed, we previously showed in rodents that meiotic and post-meiotic male germ cells lack the functional type I IFN receptor (49), and do not express ISGs after viral or IFN stimulation, unlike testicular somatic cells (56, 57). Differences in antiviral (e.g. sensing pathways and ISG induction patterns) and pro-inflammatory immune responses in human versus mouse testis may explain the testis pathogenicity observed in type I IFN-signaling deficient mouse models (along with differences in infection levels). Differences in type I IFN up-regulation following ZIKV infection may also explain the restricted tropism of ZIKV in the testis from immunocompetent mice (25) when compared to human testis explants. Whether these differences derive from intrinsic differences between human and mouse testicular cells, differential escape mechanisms mediated by ZIKV (e.g. specific counteracting of type I IFN by ZIKV in human

388 cells but not in immunocompetent mouse cells), or ex vivo/in vivo differences (e.g. infiltrating cells
389 pro-inflammatory activity) requires further investigation.

390 To date, ZIKV is the only arbovirus known to be sexually transmitted within the human
391 population. RNA from other arboviruses such as dengue, yellow fever and chikungunya viruses
392 were recently evidenced in semen from infected men for a prolonged period (58–60), but no cases
393 of sexual transmission have been documented so far. Dengue virus did not productively infect/alter
394 testicular cells in mouse models (12, 13, 25, 51) and poorly infected human Sertoli cells. Although
395 the neuro-tropic West Nile virus (WNV) replicated to levels similar to ZIKV in a Sertoli cell line
396 (27), testis from men with neuro-invasive WNV tested negative,except for one immune-suppressed
397 patient (61). Interestingly, Japanese encephalitis virus, another mosquito-borne neuro-tropic
398 flavivirus, infects the testis of boars and their semen for a long period of time, disrupts
399 spermatogenesis and can be transmitted through semen (62).

400 Of note, other male genital organs may be involved in ZIKV shedding in human semen, as
401 suggested by ZIKV prolonged sexual transmission from vasectomized men (63), and by ZIKV
402 replication in human prostate cell lines and cell lines based organoids (64). Interestingly, we
403 recently demonstrated in SIV-infected cynomolgus macaques that depending on the individuals,
404 different male genital organs may be the source of the virus in semen (65). Nevertheless, the
405 significant reduction of ZIKV titers and shorter infectivity window in semen from vasectomized
406 mice indicates the importance of testis/epididymis contributions to infectious virus shedding (4).

407 In conclusion, we demonstrated that ZIKV replicates in the human testis ex vivo and infects
408 a range of somatic cells and germ cells. Replication of ZIKV in testicular germ cells was evidenced
409 in semen from ZIKV-infected men, along with ZIKV association with spermatozoa. ZIKV had no
410 major deleterious effect on the morphology and hormonal production of the human testis in culture.
411 Despite a broad induction of antiviral genes, the absence of IFN up-regulation and minimal pro-

412 inflammatory response of the human testis ex vivo, along with the lack of ZIKV cytopathic effect
413 on testicular cells, might favour the prolonged ZIKV infection observed in this organ, and account
414 for the absence of orchitis in men infected by ZIKV. Overall, our results suggest that ZIKV
415 infection of the human testis may be involved in the persistence of the virus in semen and in altered
416 semen parameters. These results call for further investigation on the impact of ZIKV on the
417 reproductive health of ZIKV-infected men and warn against the potential horizontal and vertical
418 transmission of ZIKV through the infected germ line. Finally, the ex vivo model of ZIKV infection
419 of the human testis we developed provides a valuable tool for the testing of antiviral agents.

420

421

MATERIAL AND METHODS

Cells lines and viruses

Asian Zika virus strains isolated during the 2015 outbreak in the French Caribbean (MRS_OPY_Martinique_PaRi-2015, passaged once in Vero cells) and during the 2013 outbreak in Polynesia (H/PF/2013, passaged three times in Vero cells) were obtained from the European Virus Archive (EVA) and further propagated in VeroE6 cells for 2 additional passages. VeroE6 cells (African green monkey kidney epithelial cells) were maintained in DMEM supplemented with 10% FCS, Glutamine (2mM) and 1% penicillin/streptomycin at 37°C with 5% CO_2 (all reagents from GIBCO). To produce viral stocks, VeroE6 cells were infected at an MOI of 0.01 in serum-free medium for 2 hours, then complete medium was added to reach a final serum concentration of 5%. When cytopathic effect was evident, supernatant was centrifuged,filtered (0,45 µm), aliquoted and frozen at -80°C. The human testicular germ cell tumor (seminoma) cell line Tcam-2 (66) was kindly provided by Dr Janet Shipley (The Institute of Cancer Research, London).

Organotypic culture of human testis explants and infection

Testes were dissected into 3 mm^3 sections transferred onto 24 well plates (2 sections/well) containing 500µl of medium (DMEM/F12 supplemented with 1X nonessential amino acids, 1X ITS, 100U/ml penicillin, 100µg/ml streptomycin, 10% FCS, all from GIBCO) in the presence or absence of 10^5 $TCID_{50}$ of ZIKV (corresponding to $2.2.10^7$ to $2.9.10^7$ vRNA copies for MRS_OPY_Martinique_PaRi-2015 and 8.10^7 vRNA copies for H/PF/2013). After overnight incubation, tissue fragments were washed 3 times with PBS and transferred onto a polyethylene terephthalate insert (3µm high density pores) in 12 well plates containing 1 ml of medium. 8 hours later, the medium was changed again to further wash away potential residual virus input (time 0 for sample collection). For each experimental condition, a minimum of two wells were tested. The

447 culture was maintained up to 9 day p.i. in a humidified atmosphere containing 5% CO_2 at 37°C with
448 medium collected and fully changed every 3 days, in order to thoroughly wash input virus and
449 assess viral production dynamic. . Media were stored frozen at −80°C for vRNA and titer
450 measurement. Tissue fragments were either fixed in neutral buffered 4% formaldehyde or frozen
451 and stored at −80°C.
452
453 **Isolation and infection of testicular cells**
454 Testis fragments were incubated in digesting medium (2mg/ml hyaluronidase, 2mg/ml collagenase
455 I, 20µg/ml in DMEM/F12) for 60 minutes at 37°C under agitation (110 rpm) to dissociate
456 interstitial tissue from seminiferous tubules. After centrifugation, the seminiferous tubule pellet
457 digested by trypsin (0.25%, 5ml/g, 20 minutes at 37°C). Trypsin was inactivated and cells filtered
458 (60µm) and cultured overnight in DMEM/F12 medium supplemented with 1X nonessential amino
459 acids, 1X ITS (human insulin, human transferrin, and sodium selenite), 100U/ml penicillin,
460 100µg/ml streptomycin and 10% FCS (all from GIBCO). Primary TGCs and Tcam-2 cells were
461 incubated with ZIKV diluted in serum-free medium at a multiplicity of infection (MOI) of 1
462 (corresponding to 1.43 x 10^6 $TCID_{50}$/million cells) for 2 hours at 37°C 5% CO2. Virus was
463 removed by washing and trypsin treatment for 5 minutes at 37°C. Primary testicular cells were
464 cultured at a density of 0.5 million cells/ml in supplemented StemPro-34 (Invitrogen) as described
465 elsewhere (67). T-cam2 cells were cultured at a density of 0.1 million cells/ml in RPMI1640
466 supplemented with P/S, Glutamine (2mM) and 10% FCS (all reagents from GIBCO).
467 **Semen samples**
468 Semen was liquefied at 37°C for 30 minutes and 10µl spread on a glass slide and dried at room
469 temperature. Smears were fixed in 4% formaldehyde and stored at -20° C. Viral loads for ZIKV in
470 seminal plasma and seminal cells were 7,25 log copies/ml and 6,7 log copies/µg total RNA
471 respectively for the donor at day 7, and 7,8 log copies/ml and 7,8 log copies/2x10^6 cells respectively

472 for the donor at day 11. Patients' serology for dengue was negative and semen samples tested
473 negative for dengue in RT- PCR.
474
475 **Mice**
476 Mice lacking the type 1 interferon receptor (68) were backcrossed >10 times onto the C57BL/6
477 background (referred to as IFNAR$^{-/-}$ mice). 7-week-old male IFNAR$^{-/-}$ mice were infected through
478 the intra-peritoneal route with 10^4 $TCID_{50}$/100 µl of ZIKV (H/PF/2013) or with PBS. 5 and 9 days
479 after infection, mice were sacrificed with carbon dioxide and collected tissue either frozen at -80°C
480 or fixed in PFA 4%.
481
482 **Real-time quantitative RT-PCR**
483 Total RNA was extracted using the QIAamp vRNA (for supernatants) or RNeasy isolation kit (for
484 tissue/cells) and treated with DNase (all from Qiagen). Extracted RNA from explant supernatants
485 was subjected to RT-qPCR using GoTaq Probe 1-step RT-qPCR System (Promega). Primers and
486 probes for ZIKV described in (69) were adapted as follows: ZIKV primer forward
487 ccgctgcccaacacaag, ZIKV primer reverse ccactaacgttcttttgcagacat, ZIKV probe
488 agcctaccttgacaagcaatcagacactcaa. A standard curve with serial dilution of a known number of
489 copies of vRNA was systematically run. The relative quantification of steroidogenesis enzymes
490 mRNA (STAR, steroidogenic acute regulatory protein; CYP11A1, cytochrome P450 family 11
491 subfamily A member 1; HSD3B2, hydroxy-delta-5-steroid dehydrogenase 3 beta- and steroid delta-
492 isomerase 2; HSD17B3, hydroxysteroid 17-beta dehydrogenase 3; CYP17A1, cytochrome P450
493 family 17 subfamily A member 1) and testicular cells markers mRNA (Inhibin B; Acta2, actin alpha
494 2 smooth muscle aorta; PGK2, phosphoglycerate kinase 2; PRM2, protamine 2) was performed as
495 previously described (29).
496 Primers for innate immune response effector genes (Supplementary Table 1) were designed using
497 Primer-BLAST tool (70). Total RNA was reverse-transcribed using the Iscript cDNA Synthesis Kit

(Bio-Rad). QPCR reactions were performed on a Bio-Rad Laboratories CFX384 instrument using iTaq SYBR green mix (BioRad) and 40 cycles of 15 seconds at 95°C and 1 minute at 60° C, followed by melt-curve analysis. Gene expression fold changes were calculated with the $2^{-\Delta\Delta Ct}$ method normalized to beta-actin and mock-infected samples expression levels.

Determination of viral titer

Vero E6 cells seeded in opaque-walled 96 well plates at a final concentration of 1,5x 10^5 cells/ml in DMEM with 5% FCS were put in contact the next day with serial dilutions of supernatant . Median tissue culture infective dose ($TCID_{50}$)/ml was measured at day 5 post-infection using the Viral ToxGlo Assay (Promega).

Histology, RNAscope in situ hybridization (ISH) and immunohistochemistry (IHC)

Tissues or cell pellets were fixed in 4% formaldehyde and embedded in paraffin. RNA ISH was performed using RNAscope 2.5 (Advanced Cell Diagnostics) according to the manufacturer's instructions, as previously described (15, 87). RNAScope ISH is a highly specific and sensitive technique, with the ability to detect single molecules (73). Formaldehyde fixed paraffin-embedded tissue sections or cell pellets were deparaffinized in xylene and deshydrated in ethanol. with for 10 min at room temperature. Slides deparaffinized and H_2O_2 quenched for endogenous peroxidases were boiled in RNAscope Target Retrieval Reagents (citrate buffer10mM, pH6, 15 minutes) and incubated in RNAscope Protease Plus (40°C, 20 minutes), prior to probe hybridization. Sections were incubated with target probes (2 hours, 40°C), washed in buffer and incubated with amplification reagents. Chromogenic detection was performed using Fast Red as substrate for alkaline phosphatase to generate red signal. Slides were counterstained with hematoxylin and mounted in Eukitt (O. KINDLER) before observation using bright-field microscopy. The "double *Z*" probes targeting ZIKV RNA (consensus sequence, target region 219-5443, catalog #467771), positive (targeting the 2514-3433 region of human *POLR2A* gene, catalog #310451) and negative

(targeting the 414-862 region of bacterial *dapB* gene, catalog #310043) control probes were all obtained from Advanced Cell Diagnostics. Staining specificity was verified as showed in Figure S3. FigureSections of ZIKV-infected Vero cell pellets and mock-infected testis tissues were systematically used as positive and negative controls.

Dual fluorescent ISH-IHC experiments was performed essentially as we previously described (74). Briefly, tissue sections were first submitted to ISH, then blocked in PBS/BSA 2% and incubated overnight at 4°C with primary antibody, Sections were washed, incubated with either anti-mouse or anti-rabbit Alexa-488 fluorescent secondary antibodies diluted 1/500 (chicken anti-mouse 488 ref A21200, chicken anti-rabbit 488 ref A21441, Life Technologies), and counterstained with Prolong medium containing DAPI before observation with a Zeiss Axio Imager M1 fluorescence microscope connected to a digital camera (Carl Zeiss) using Zen software. Fluorescent Fast Red signal was read at 550 nm.

Single immunohistochemistry was performed as described (75). For immunofluorescence experiments, Alexa 488 or 594-coupled secondary antibodies diluted 1/500 (goat anti-mouse 594 ref A11032, chicken anti-rabbit 594 ref A21442, donkey anti-rat 488 ref A21208, all from Life Technologies) were used and sections mounted with Prolong DAPI to stain the nuclei. Cell staining was never observed for isotypic controls or mock-infected samples. Primary antibodies used : mouse anti-NS1 (Biofront Technologies, clone 0102136, 4µg/ml), anti-CD68 (DAKO, clone KP1, 1,85µg/ml), anti-CD163 (LEICA Novocastra, clone 10D6, 1/100), anti- αSMA (DAKO, clone 1A4, 1,4µg/ml), anti-DDX4 (GENETEX, clone 2F9H5, 1/200), anti-ZO-1 (THERMO FISHER, clone ZO1-1A12, 10µg/ml); rabbit anti-Cyp11A1 (Sigma, 1/250), anti-cleaved caspase 3 (Cell Signaling, Asp175, 1/50), anti-DDX4 (Abcam, 2µg/ml), anti-STAR (Cell signalling, 1/200), anti-CD3 (Dako, #A0452, 10 µg/ml); rat anti-mouse F4/80 (Abcam, clone BM8, 1/20).

The number of ZIKV RNA+ CD68/CD163+ macrophages, CYP11A+ Leydig cells, αSMA+ peritubular cells, germ cells and Sertoli cells (identified on morphological criteria in light

549 microscopy) in testis explants was assessed in 4 donors and at least 3 whole testis tissue
550 sections/donors (corresponding to about 12 mm^2/ testis donor). Quantification of CD3+ cells in
551 mouse testis was performed in 3 mock-infected animals, 4 animals at day 5 p.i. and 4 animals at day
552 9 p.i., in at least 5 mm^2/testis. Slides were scanned with a NanoZoomer slide scanner (Hamamatsu
553 Photonics, France, at Plateforme H2P2, Biosit, Rennes, France). Immunostained positive cells were
554 counted with ImageJ free software.
555
556 **Immunocytofluorescence**
557 Semen smears from donors and cell pellets from testicular cell cultures put onto polylysine-coated
558 glass coverslips were fixed in 4% PAF for 20 minutes at RT. After permeabilization (0,2% Triton
559 X-100, 10 minutes), the slides were incubated in blocking buffer (0,2% Triton X-100, 1% goat
560 serum, 2 hours) and stained with antibodies against ZIKV NS1 (1:1000, Biofront Technologies) or
561 flavivirus envelope Ab 4G2 (1:1000, Millipore). NS1 antibody was either directly coupled to Alexa
562 Fluor 647 (Zenon labeling kit, Molecular Probes) or revealed using Alexa-fluor 555 goat anti-
563 mouse (Life Technologies). Infected cell characterization was performed using rabbit anti-DDX4
564 (5µg/ml, Abcam), anti-Stra8 (9,6µg/ml, ThermoFisher Scientific) and anti-FSHR (10µg/ml,
565 Origene), detected using Alexa-fluor 488 (Invitrogen) or Alexa-fluor 647 goat anti-rabbit (Jackson
566 Immunoresearch), mouse anti-MageA4 (clone 57B, 4µg/ml) coupled to Alexa Fluor 647 (Zenon
567 labeling kit, Molecular Probes), and mouse anti-αSMA (clone 1A4, 0,5µg/ml, Dako) detected using
568 Alexa-fluor 555 goat-anti mouse antibody. Isotype control antibodies or non- infected cells were
569 used as negative controls. Slides were counterstained with Prolong medium containing DAPI
570 (Molecular Probes). Images were acquired with the SP8 confocal system (Leica) connected to LAS
571 software or with DMRXA wide field microscope (Applied Precision), and analyzed using Fiji
572 software.
573

Testosterone and inhibin B immunoassays

Testosterone was assayed using a specific radioimmunoassay (Immunotech, Beckman Coulter). Inhibin B was assayed using a commercial enzyme-linked immunosorbent assay (ELISA) kit (DSL-10-84100 Active, Beckman Coulter).

Viability assay

Cell viability was assessed by measuring the release of lactate dehydrogenase (LDH) using the enzymatic fluorimetric assay CytoTox-ONE™ Homogeneous Membrane Integrity Assay (Promega).

Cytokine release measurement

A bead-based multiplex flow cytometry Legendplex assay (Biolegend, Ozyme) was used. Fluorescence was read using the BD LSRII Fortessa flow cytometer.

Statistics

Data were analyzed with non-parametric paired Friedman-Dunn's or unpaired Kruskal-Wallis-Dunn's test when more than 2 sets of samples were compared, as specified in figure legends. The non-parametric Mann-Whitney test was used to analyze differences in viral load of mice testis at day 5 and 9 post infection. Correlations were calculated using the Spearman test. Values were considered significant when $P<0,05$. Statistical analyses were performed using commercially-available software (GraphPadPrism 6, GraphPad Software, Inc., La Jolla, California, USA).

Study approval

Normal testes were obtained either after orchidectomy from prostate cancer patients who had not received any hormone therapy or at autopsy, and processed within 2 hours of surgery. The

599 procedure was approved by a local ethics committee (authorization #DC-2016-2783) and the French
600 national agency for biomedical research (authorization #PF S09-015).
601 Semen samples were obtained by masturbation from two ZIKV-infected donors living in the French
602 Caribbean at 7 and 11 days post-symptoms onset respectively, after informed consent was obtained,
603 in the French Cohort of Patients Infected by an Arbovirus (CARBO; ClinicalTrials.gov identifier
604 NCT01099852).
605 Mice were housed at the Institut Pasteur Animal Facility accredited by the French Ministry of
606 Agriculture for performing experiments on live rodents. Work on animals was performed in
607 compliance with French and European regulations on care and protection of laboratory animals (EC
608 Directive 2010/63, French Law 2013-118, February 6th, 2013). All experiments with $IFNAR^{-/-}$
609 mice were approved by the Ethics Committee #89 and registered under the reference #2016-0018.
610
611

AUTHOR CONTRIBUTIONS

GM performed experiments, analyzed data, co-wrote the paper and contributed to data interpretation and study design. LH, APS, DM, FA and ALT performed experiments, analyzed data and contributed to writing the paper. LH designed primers and interpreted PCR array results. JF and SB performed experiments. GA interpreted data. KB and SL contributed testis tissues. GJ, LB and AC contributed semen samples. TC and ML performed IFNAR mouse infection and tissue collection. NDR designed experiments, interpreted the data and wrote the paper.

All authors read, edited and approved the manuscript.

ACKNOWLEDGEMENTS

This project received funding from the European Union's Horizon 2020 research and innovation program under grant agreement no. 733176, ZIKAPLAN (grant agreement no. 734584) and ZIKALLIANCE (grant agreement no. 734548) and was funded in part by the LabEx IBEID, Institut Pasteur and Inserm. GM received support from REACTing. GA and NDR received funding from CAPES-COFECUB. GJ and LB received funding from Agence de la Biomédecine and Agence Régionale de santé Guadeloupe for the collection of semen from infected men. AC received funding from the French Ministry of Health (Soutien Exceptionnel à la Recherche et à l'Innovation) and support from REACTing. Experiments were conducted in part on L3, MRic and H2P2 platforms at Biosit federative structure (Univ Rennes, CNRS, Inserm, BIOSIT [(Biologie, Santé, Innovation Technologique de Rennes)] - UMS 3480, US_S 018). This publication was supported by the European Virus Archive goes Global (EVAg) project that has received funding from the European Union's Horizon 2020 research and innovation program under grant agreement N°653316. We thank Xavier Montagutelli for his help with animal experiment and Laurianne Lesné and Christèle Desdoits for their assistance in hormonal assays.

REFERENCES

1. Coelho FC et al. Higher incidence of Zika in adult women than adult men in Rio de Janeiro suggests a significant contribution of sexual transmission from men to women. *Int. J. Infect. Dis.* 2016;51:128–132.
2. Yakob L, Kucharski A, Hue S, Edmunds WJ. Low risk of a sexually-transmitted Zika virus outbreak. *Lancet Infect. Dis.* 2016;16(10):1100–1102.
3. Moreira J, Peixoto TM, Siqueira AM, Lamas CC. Sexually acquired Zika virus: a systematic review. *Clin. Microbiol. Infect.* 2017;23(5):296–305.
4. Duggal NK et al. Frequent Zika Virus Sexual Transmission and Prolonged Viral RNA Shedding in an Immunodeficient Mouse Model. *Cell Rep.* 2017;18(7):1751–1760.
5. Haddow AD et al. High Infection Rates for Adult Macaques after Intravaginal or Intrarectal Inoculation with Zika Virus. *Emerg. Infect. Dis.* 2017;23(8):1274–1281.
6. Carroll T et al. Zika virus preferentially replicates in the female reproductive tract after vaginal inoculation of rhesus macaques. *PLOS Pathog.* 2017;13(7):e1006537.
7. Tang WW et al. A Mouse Model of Zika Virus Sexual Transmission and Vaginal Viral Replication. *Cell Rep.* 2016;17(12):3091–3098.
8. Duggal NK, McDonald EM, Ritter JM, Brault AC. Sexual transmission of Zika virus enhances in utero transmission in a mouse model. *Sci. Rep.* 2018;8(1):4510.
9. Epelboin S et al. Zika virus and reproduction: facts, questions and current management. *Hum. Reprod. Update* 2017;23(6):629–645.
10. Barzon L et al. Virus and Antibody Dynamics in Travelers With Acute Zika Virus Infection. *Clin. Infect. Dis.* 2018;66(8):1173–1180.
11. Mead PS et al. Zika Virus Shedding in Semen of Symptomatic Infected Men. *N. Engl. J. Med.* 2018;378(15):1377–1385.
12. Govero J et al. Zika virus infection damages the testes in mice. *Nature* 2016;540(7633):438–442.
13. Ma W et al. Zika Virus Causes Testis Damage and Leads to Male Infertility in Mice. *Cell* 2016;167(6):1511–1524 e10.
14. Griffin BD et al. DNA vaccination protects mice against Zika virus-induced damage to the testes. *Nat. Commun.* 2017;8:15743.
15. Shan C et al. A single-dose live-attenuated vaccine prevents Zika virus pregnancy transmission and testis damage. *Nat. Commun.* 2017;8(1):676.
16. Osuna CE et al. Zika viral dynamics and shedding in rhesus and cynomolgus macaques. *Nat. Med.* 2016;22(12):1448–1455.
17. Hirsch AJ et al. Zika Virus infection of rhesus macaques leads to viral persistence in multiple tissues. *PLOS Pathog.* 2017;13(3):e1006219.
18. Koide F et al. Development of a Zika Virus Infection Model in Cynomolgus Macaques. *Front. Microbiol.* 2016;7:2028.
19. Joguet G et al. Effect of acute Zika virus infection on sperm and virus clearance in body fluids: a prospective observational study. *Lancet Infect. Dis.* 2017;17(11):1200–1208.
20. Roulet V et al. Human testis in organotypic culture: application for basic or clinical research. *Hum Reprod* 2006;21(6):1564–1575.
21. Young JC et al. TCam-2 seminoma cell line exhibits characteristic foetal germ cell responses to TGF-beta ligands and retinoic acid. *Int. J. Androl.* 2011;34(4pt2):e204–e217.
22. Uraki R et al. Zika virus causes testicular atrophy. *Sci. Adv.* 2017;3(2):e1602899.
23. Xia Y, Zhu WJ, Hao SF, Liang WB, Li J. Stereological analysis of age-related changes of testicular peritubular cells in men. *Arch. Gerontol. Geriatr.* 2012;55(1):116–119.
24. Nieschlag E, Behre HM (eds). *Andrology*. Verlag Berlin Heidelberg: Springer; 2010.
25. Robinson CL et al. Male germ cells support long-term propagation of Zika virus. *Nat. Commun.* 2018;9(1):2090.

688 26. Mansuy JM et al. Zika virus in semen and spermatozoa. *Lancet Infect. Dis.* 2016;16(10):1106–
689 1107.
690 27. Siemann DN, Strange DP, Maharaj PN, Shi P-Y, Verma S. Zika Virus Infects Human Sertoli
691 Cells and Modulates the Integrity of the *In Vitro* Blood-Testis Barrier Model. *J. Virol.*
692 2017;91(22):e00623-17.
693 28. Kumar A et al. Human Sertoli cells support high levels of Zika virus replication and persistence.
694 *Sci. Rep.* 2018;8(1):5477.
695 29. Kristensen DM et al. Ibuprofen alters human testicular physiology to produce a state of
696 compensated hypogonadism. *Proc. Natl. Acad. Sci.* 2018;115(4):E715–E724.
697 30. Adamopoulos DA, Lawrence DM, Vassilopoulos P, Contoyiannis PA, Swyer GI. Pituitary-
698 testicular interrelationships in mumps orchitis and other viral infections. *Br-Med-J*
699 1978;1(6121):1177–1447.
700 31. Potter SJ, DeFalco T. Role of the testis interstitial compartment in spermatogonial stem cell
701 function. *Reproduction* 2017;153(4):R151–R162.
702 32. Cheng CY, Wong EW, Yan HH, Mruk DD. Regulation of spermatogenesis in the
703 microenvironment of the seminiferous epithelium: new insights and advances. *Mol Cell Endocrinol*
704 2010;315(1–2):49–56.
705 33. Mayerhofer A. Human testicular peritubular cells: more than meets the eye. *Reproduction*
706 2013;145(5):R107–R116.
707 34. Huits R et al. Zika virus in semen: a prospective cohort study of symptomatic travellers
708 returning to Belgium. *Bull. World Health Organ.* 2017;95(12):802–809.
709 35. Sergerie M, Mieusset R, Croute F, Daudin M, Bujan L. High risk of temporary alteration of
710 semen parameters after recent acute febrile illness. *Fertil. Steril.* 2007;88(4):970.e1-7.
711 36. Evenson DP, Jost LK, Corzett M, Balhorn R. Characteristics of human sperm chromatin
712 structure following an episode of influenza and high fever: a case study. *J. Androl.* 2000;21(5):739–
713 46.
714 37. Quicke KM et al. Zika Virus Infects Human Placental Macrophages. *Cell Host Microbe*
715 2016;20(1):83–90.
716 38. Mladinich MC, Schwedes J, Mackow ER. Zika Virus Persistently Infects and Is Basolaterally
717 Released from Primary Human Brain Microvascular Endothelial Cells. *MBio* 2017;8(4):e00952-17.
718 39. Strange DP, Green R, Siemann DN, Gale M, Verma S. Immunoprofiles of human Sertoli cells
719 infected with Zika virus reveals unique insights into host-pathogen crosstalk. *Sci. Rep.*
720 2018;8(1):8702.
721 40. Strange DP et al. Human testicular organoid system as a novel tool to study Zika virus
722 pathogenesis. *Emerg. Microbes Infect.* 2018;7(1):82.
723 41. Singh PK et al. Zika virus infects cells lining the blood-retinal barrier and causes chorioretinal
724 atrophy in mouse eyes. *JCI insight* 2017;2(4):e92340.
725 42. Van der Hoek KH et al. Viperin is an important host restriction factor in control of Zika virus
726 infection. *Sci. Rep.* 2017;7(1):4475.
727 43. Savidis G et al. The IFITMs Inhibit Zika Virus Replication. *Cell Rep.* 2016;15(11):2323–2330.
728 44. Perelygin AA et al. Positional cloning of the murine flavivirus resistance gene. *Proc. Natl.*
729 *Acad. Sci.* 2002;99(14):9322–9327.
730 45. Chen J et al. Outcomes of Congenital Zika Disease Depend on Timing of Infection and
731 Maternal-Fetal Interferon Action. *Cell Rep.* 2017;21(6):1588–1599.
732 46. Schoggins JW et al. A diverse range of gene products are effectors of the type I interferon
733 antiviral response. *Nature* 2011;472(7344):481–485.
734 47. Ngono AE, Shresta S. Immune Response to Dengue and Zika. *Annu. Rev. Immunol.*
735 2018;36(1):annurev-immunol-042617-053142.
736 48. Xia H et al. An evolutionary NS1 mutation enhances Zika virus evasion of host interferon
737 induction. *Nat. Commun.* 2018;9(1):414.
738 49. Satie AP et al. Excess type I interferon signaling in the mouse seminiferous tubules leads to

739 germ cell loss and sterility. *J Biol Chem* 2011;286(26):23280–23295.
740 50. Hasan M et al. Trex1 regulates lysosomal biogenesis and interferon-independent activation of
741 antiviral genes. *Nat. Immunol.* 2012;14(1):61–71.
742 51. Sheng Z-Y et al. Sertoli Cells Are Susceptible to ZIKV Infection in Mouse Testis. *Front. Cell.*
743 *Infect. Microbiol.* 2017;7:272.
744 52. Chan JF-W et al. Zika Virus Infection in Dexamethasone-immunosuppressed Mice
745 Demonstrating Disseminated Infection with Multi-organ Involvement Including Orchitis Effectively
746 Treated by Recombinant Type I Interferons. *EBioMedicine* 2016;14:112–122.
747 53. Winkler CW et al. Adaptive Immune Responses to Zika Virus Are Important for Controlling
748 Virus Infection and Preventing Infection in Brain and Testes. *J. Immunol.* 2017;198(9):3526–3535.
749 54. Dejucq N, Lienard MO, Guillaume E, Dorval I, Jegou B. Expression of interferons-alpha and -
750 gamma in testicular interstitial tissue and spermatogonia of the rat. *Endocrinology*
751 1998;139(7):3081–3087.
752 55. Le Tortorec A et al. Antiviral responses of human Leydig cells to mumps virus infection or poly
753 I:C stimulation. *Hum Reprod* 2008;23(9):2095–2103.
754 56. Dejucq N, Lienard MO, Jegou B. Interferons and interferon-induced antiviral proteins in the
755 testis. *J Reprod Immunol* 1998;41(1–2):291–300.
756 57. Dejucq N, Chousterman S, Jegou B. The testicular antiviral defense system: localization,
757 expression, and regulation of 2'5' oligoadenylate synthetase, double-stranded RNA-activated
758 protein kinase, and Mx proteins in the rat seminiferous tubule. *J Cell Biol* 1997;139(4):865–873.
759 58. Lalle E et al. Prolonged detection of dengue virus RNA in the semen of a man returning from
760 Thailand to Italy, January 2018. *Eurosurveillance* 2018;23(18). doi:10.2807/1560-
761 7917.ES.2018.23.18.18-00197
762 59. Barbosa CM et al. Yellow Fever Virus DNA in Urine and Semen of Convalescent Patient,
763 Brazil. *Emerg. Infect. Dis.* 2018;24(1):176–178.
764 60. Bandeira AC et al. Prolonged shedding of Chikungunya virus in semen and urine: A new
765 perspective for diagnosis and implications for transmission. *IDCases* 2016;6:100–103.
766 61. Armah HB et al. Systemic distribution of West Nile virus infection: postmortem
767 immunohistochemical study of six cases. *Brain Pathol.* 2007;17(4):354–62.
768 62. Guérin B, Pozzi N. Viruses in boar semen: detection and clinical as well as epidemiological
769 consequences regarding disease transmission by artificial insemination. *Theriogenology*
770 2005;63(2):556–72.
771 63. Stassen L, Armitage C, van der Heide D, Beagley K, Frentiu F. Zika Virus in the Male
772 Reproductive Tract. *Viruses* 2018;10(4):198.
773 64. Spencer JL et al. Replication of Zika Virus in Human Prostate Cells: A Potential Source of
774 Sexually Transmitted Virus. *J. Infect. Dis.* 2018;217(4):538–547.
775 65. Houzet L et al. Seminal SIV in chronically-infected cynomolgus macaques is dominated by
776 virus originating from multiple genital organs. *J. Virol.* 2018;JVI.00133-18.
777 66. Mizuno Y, Gotoh A, Kamidono S, Kitazawa S. [Establishment and characterization of a new
778 human testicular germ cell tumor cell line (TCam-2)]. *Nihon Hinyokika Gakkai Zasshi.*
779 1993;84(7):1211–8.
780 67. Sadri-Ardekani H et al. Propagation of Human Spermatogonial Stem Cells In Vitro. *JAMA*
781 2009;302(19):2127.
782 68. Müller U et al. Functional role of type I and type II interferons in antiviral defense. *Science*
783 1994;264(5167):1918–21.
784 69. Lanciotti RS et al. Genetic and Serologic Properties of Zika Virus Associated with an Epidemic,
785 Yap State, Micronesia, 2007. *Emerg. Infect. Dis.* 2008;14(8):1232–1239.
786 70. Ye J et al. Primer-BLAST: A tool to design target-specific primers for polymerase chain
787 reaction. *BMC Bioinformatics* 2012;13(1):134.
788 71. Wang F et al. RNAscope: a novel in situ RNA analysis platform for formalin-fixed, paraffin-
789 embedded tissues. *J. Mol. Diagnostics* 2012;14(1):22–29.

790 72. Deleage C et al. Defining HIV and SIV Reservoirs in Lymphoid Tissues. *Pathog. Immun.*
791 2016;1(1):68–106.
792 73. Deleage C, Chan CN, Busman-Sahay K, Estes JD. Next-generation in situ hybridization
793 approaches to define and quantify HIV and SIV reservoirs in tissue microenvironments.
794 *Retrovirology* 2018;15(1):4.
795 74. Matusali G et al. Detection of Simian Immunodeficiency Virus in Semen, Urethra, and Male
796 Reproductive Organs during Efficient Highly Active Antiretroviral Therapy. *J Virol*
797 2015;89(11):5772–5787.
798 75. Roulet V et al. Susceptibility of human testis to human immunodeficiency virus-1 infection in
799 situ and in vitro. *Am J Pathol* 2006;169(6):2094–2103.
800

801

802 **FIGURES AND FIGURE LEGENDS**

803

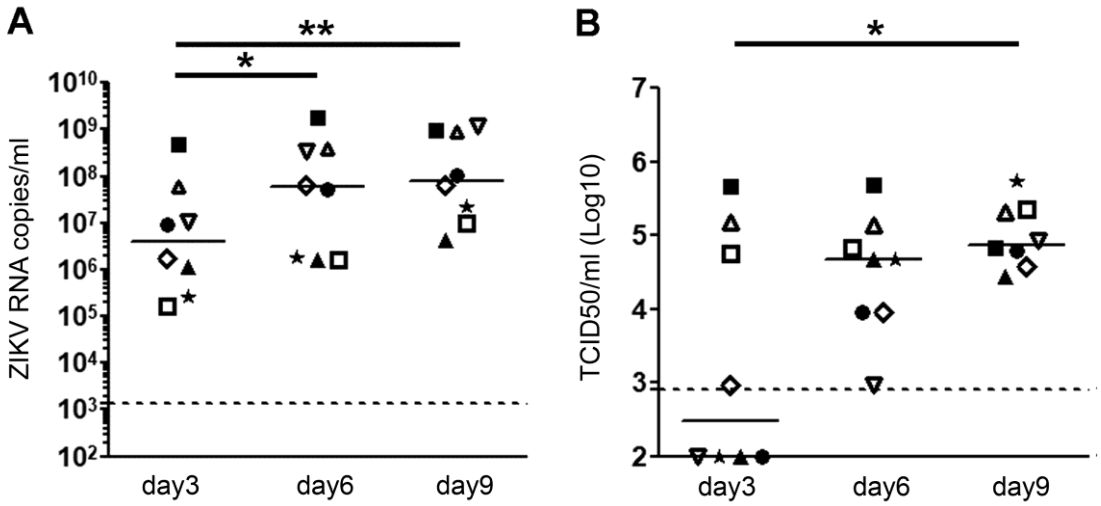

804

805

806 **Figure 1 ZIKA virus replicates in human testicular tissue**. Human testis explants from 8 donors
807 were ex vivo infected overnight with 10^5 $TCID_{50}$ (corresponding to $2.2.10^7$ to $2.9.10^7$ vRNA copies)
808 from a low-passage ZIKV strain isolated in 2015 in the French Caribbean
809 (MRS_OPY_Martinique_PaRi-2015). Explants were thoroughly washed and cultured on inserts in
810 1 ml of medium/well for 9 days, with media fully removed and changed every 3 days. Each of the
811 time points (day 3, day 6, day 9) represent de novo viral release over a 3-day-culture period. A)
812 ZIKV RNA release over a 3-day-culture period at day 3, day 6 and day 9 detected by RT-qPCR; B)
813 Viral titers determined by infectivity assay of 3-day-culture period tissue supernatants on VeroE6
814 cells. Each symbol represents a different donor (same symbol/donor throughout the manuscript
815 figures). Dotted lines represent the detection limit of the assays. Mock-infected explants were
816 always below detection level. Bars represent median. *P<0,05; **P<0,01 (Friedman-Dunns non-
817 parametric comparison).

818

819

820

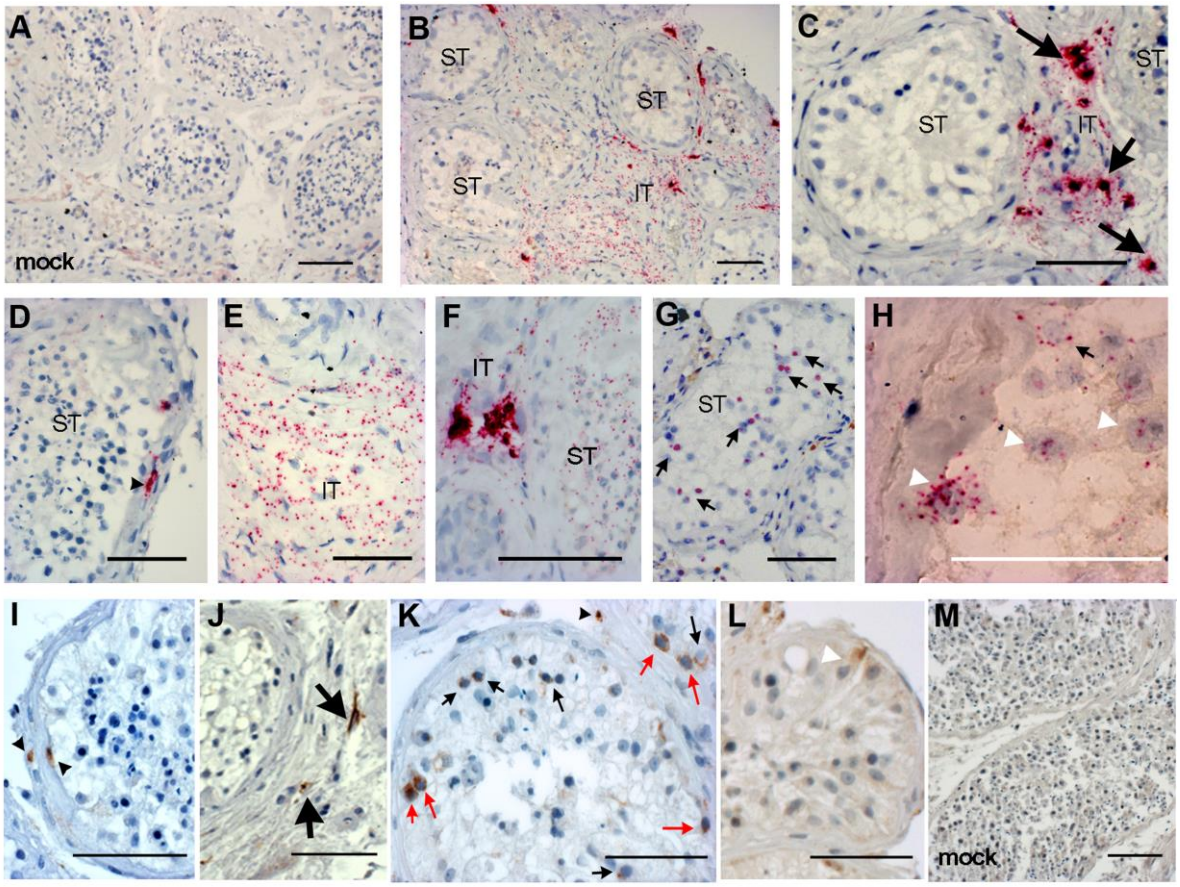

Figure 2 ZIKV infects somatic and germ cells in human testis explants.
A-H) Representative images of RNAscope in situ hybridization for ZIKV RNA in control mock-infected (A) and ZIKV-infected testis explant (n=8 independent donors) after 6 days of culture (B-H). ZIKV RNA labeling was observed in the interstitial tissue (IT) of testis explants (B, C, E, F), in cells bordering the seminiferous tubules (ST) (B, D) and within seminiferous tubules (F,G,H). I-M) Representative images of immunohistochemistry staining of NS1-ZIKV performed on ZIKV-infected (I-L) and mock-infected (M) testis explants in culture for 6 days (n=8 independent donors). Black arrow heads point at infected cells in the extracellular matrix surrounding the seminiferous tubules. Thick arrows point at infected cells in the interstitial tissue. Thin black arrows point at infected germ cells. Thin red arrows point at infected spermatogonia. White arrow heads point at Sertoli cell nucleus. Black scale bars=100µm; White bar=50µm.

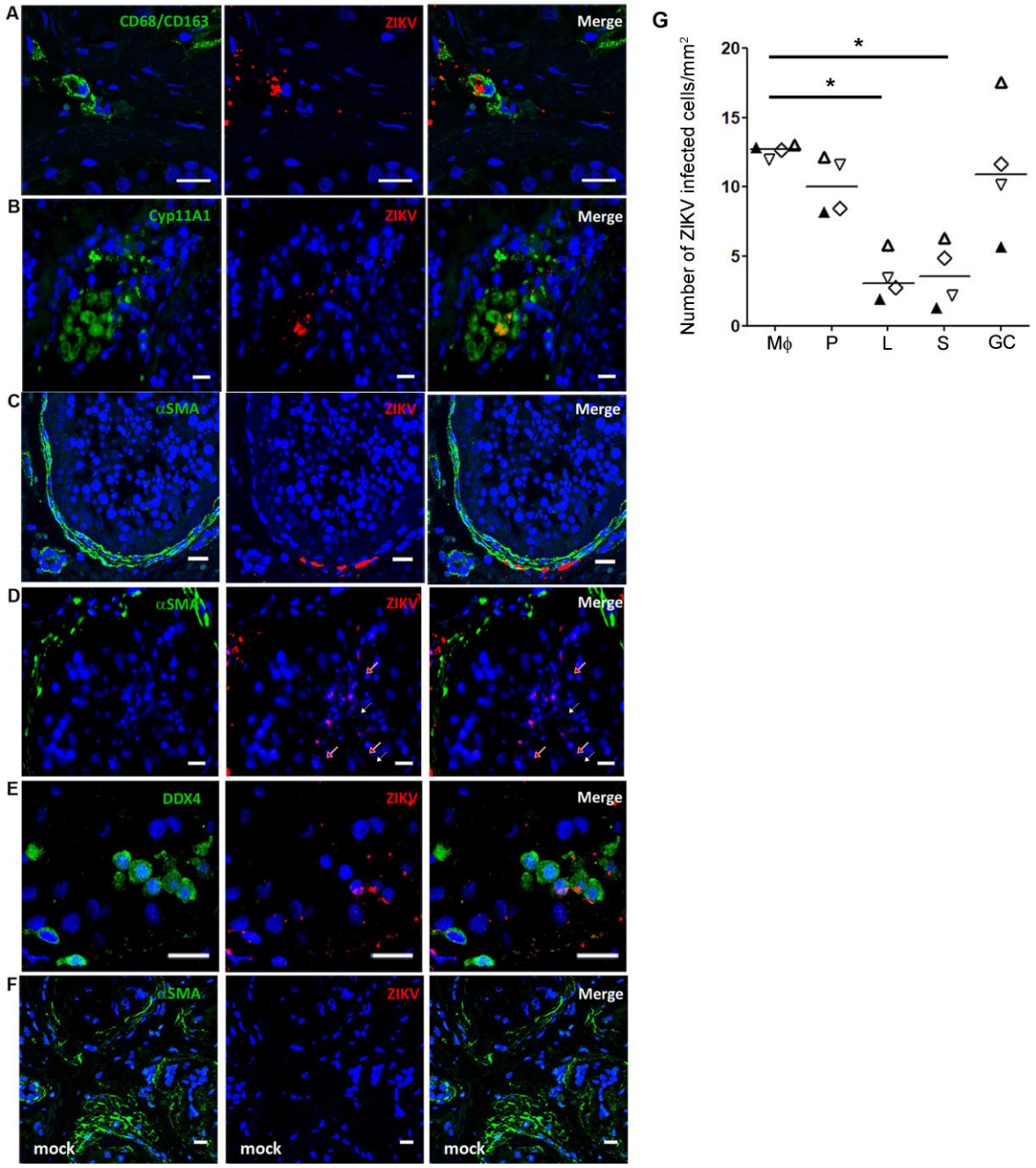

Figure 3 Characterization and quantification of ZIKV-infected human testicular cells ex vivo. RNAscope in situ hybridization for vRNA coupled with immunofluorescence for cell markers identified ZIKV RNA in CD68/CD163+ macrophages (A), Cyp11A1+ Leydig cells (B), αSMA+ peritubular cells (C), late germ cells localized near the lumen in seminiferous tubules (white arrows: round spermatids; red arrows: elongated spermatids) (D) and DDX4+ early germ cells (E). Staining for ZIKV was never observed in mock-infected testis (F). Nuclei are stained in blue. Scale bars=20µm. (G) Infected cells were quantified in at least 3 whole tissue sections from 4 testis donors (each represented by a different symbol) at day 9 p.i. Mϕ: macrophages; P: peritubular cells; L: Leydig cells; S: Sertoli cells; GC: germ cells. Bars represent median. *P<0,05 (Friedman-Dunns non parametric comparison).

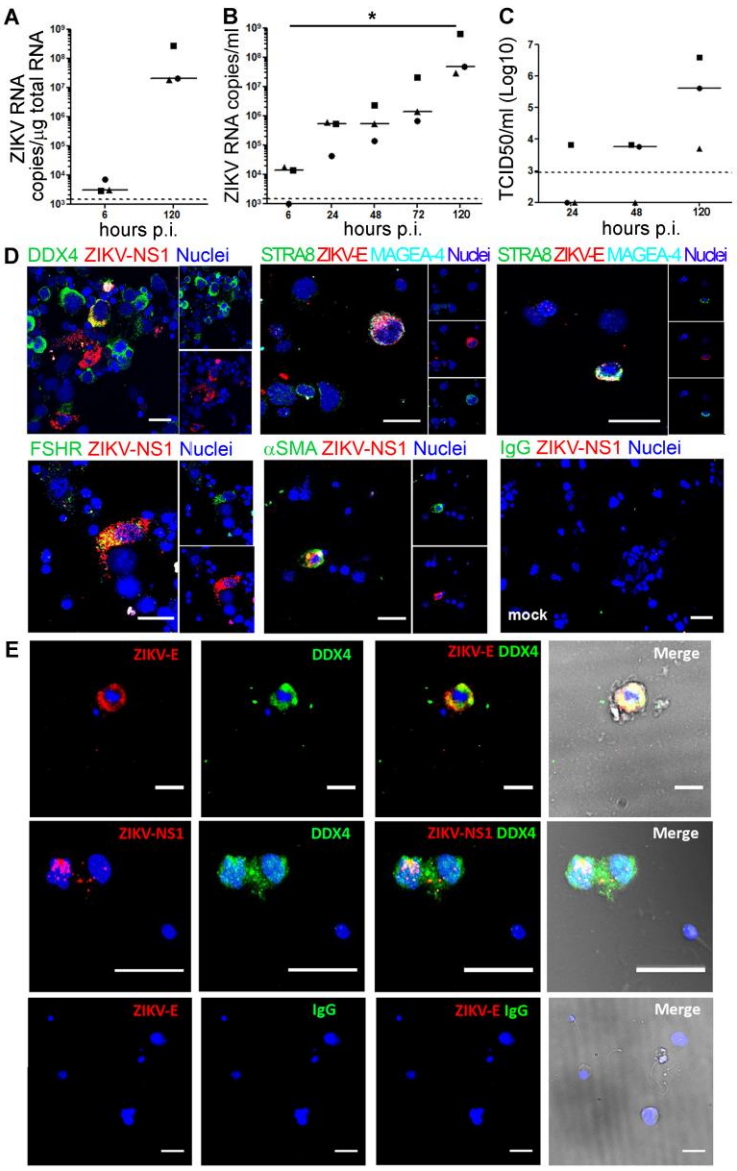

Figure 4 ZIKV replicates in human testicular germ cells in vitro and in vivo. A-C) Primary testicular cells were infected with ZIKV (MOI 1, corresponding to 7.15 x 10^5 $TCID_{50}$ units/ ml/ 0.5 million cells). ZIKV RNA detected by RT-qPCR in cells (A) and culture supernatants (B). C) Viral titers determined by infectivity assay of tissue supernatants on VeroE6 cells. Each dot represents independent donors. Bars represent median values. Dotted lines indicate detection limit. *P<0,05 (Friedman-Dunns non-parametric comparison). D) Immunofluorescence against ZIKV NS1 or envelope (ZIKV-E) proteins combined with cell markers for all germ cells (DDX4) or specific germ cell types (STRA8, MAGEA4), Sertoli cells (FSH-R) and peritubular cells (αSMA). Nuclei are stained in blue. E) Detection of infected germ cells in semen from ZIKV-infected men. Immunofluorescent labelling of semen cell smears from two ZIKV-infected patients, one at day 7 (top panel) and one at day 11 (middle panel) post-symptoms onset. ZIKV Envelope (ZIKV-E) or NS1 protein co-labelled with the germ cell marker DDX4. Bottom panels show semen from a healthy individual stained with anti- ZIKV-E antibody and IgG isotype as a negative control. Nuclei are stained in blue. In the merge panels, brightfield images are included to visualize the cell's morphology. Scale bars=20µm.

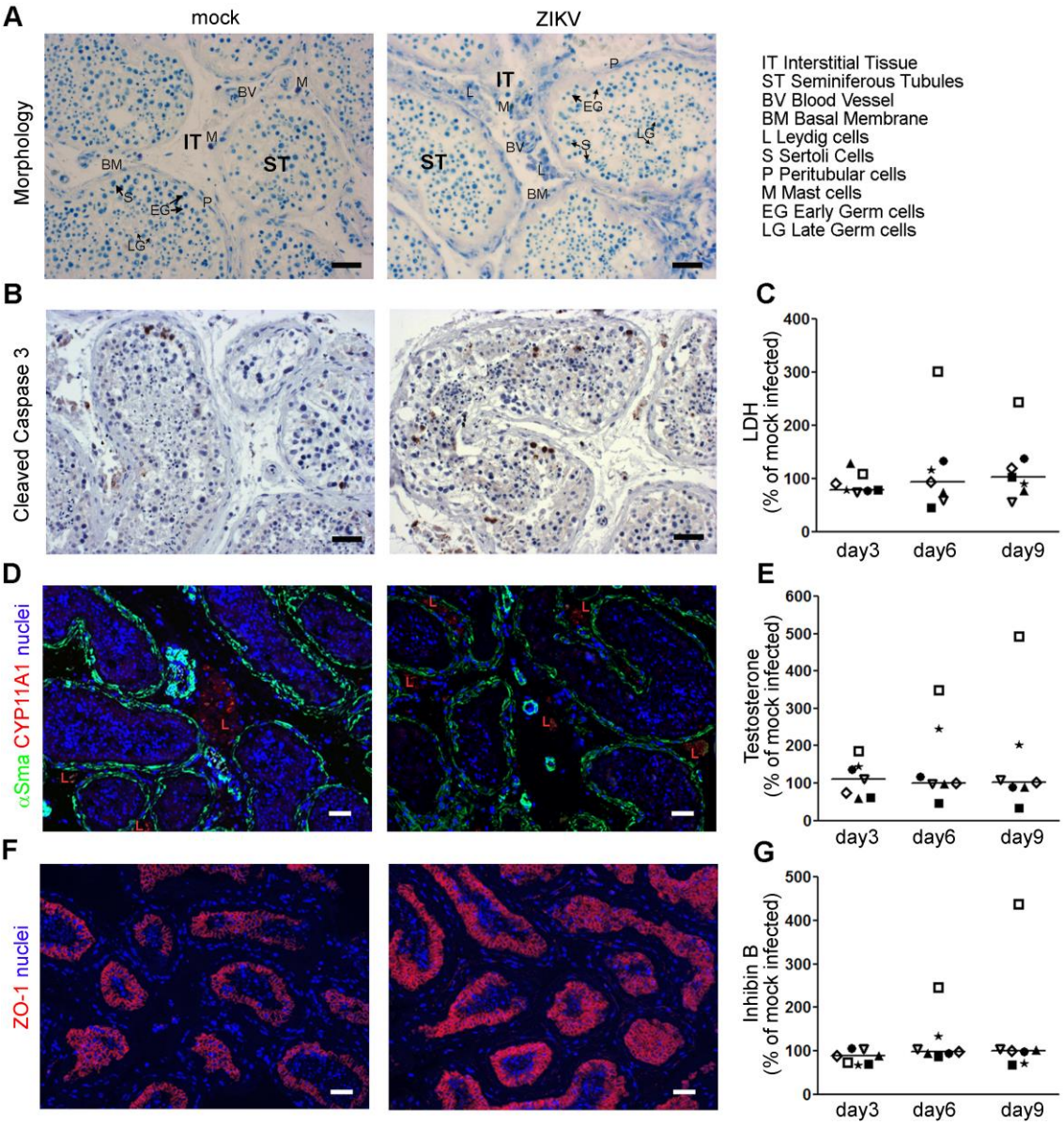

Figure 5 ZIKV infection ex vivo does not alter human testis explant morphology, cell viability or hormonal production. A) Toluidine histological staining of testis explants, shown here for mock- infected (left panel) and ZIKV-infected (right panel) testis explants at day 6 post-infection (p.i.). B) Cleaved caspase 3 IHC to detect apoptotic cells in mock (left panel) and ZIKV-infected (right panel) testis explants, shown here for day 6 p.i. C) Lactate dehydrogenase (LDH) release in testis supernatant expressed as % of mock-infected explants at the corresponding day of culture. D) Immuno-fluorescent co-labeling of peritubular (αSMA) and Leydig (Cyp11A1) cells, shown on tissue sections at day 6 p.i. for mock (left panel) and ZIKV-infected (right panel) explants. Nuclei are stained in blue. E, G) Testosterone and inhibin B release in testis supernatants expressed as % of mock-infected explants at the corresponding day of culture. F) Immuno-fluorescent labeling of Sertoli cells tight junctions associated protein ZO-1 in tissues sections for mock (left panel) and ZIKV-infected (right panel) explants, shown at day 6 p.i. Nuclei are stained in blue. Bars=50µm. C, E, G: each symbol represents a different donor; horizontal bars represent median values.

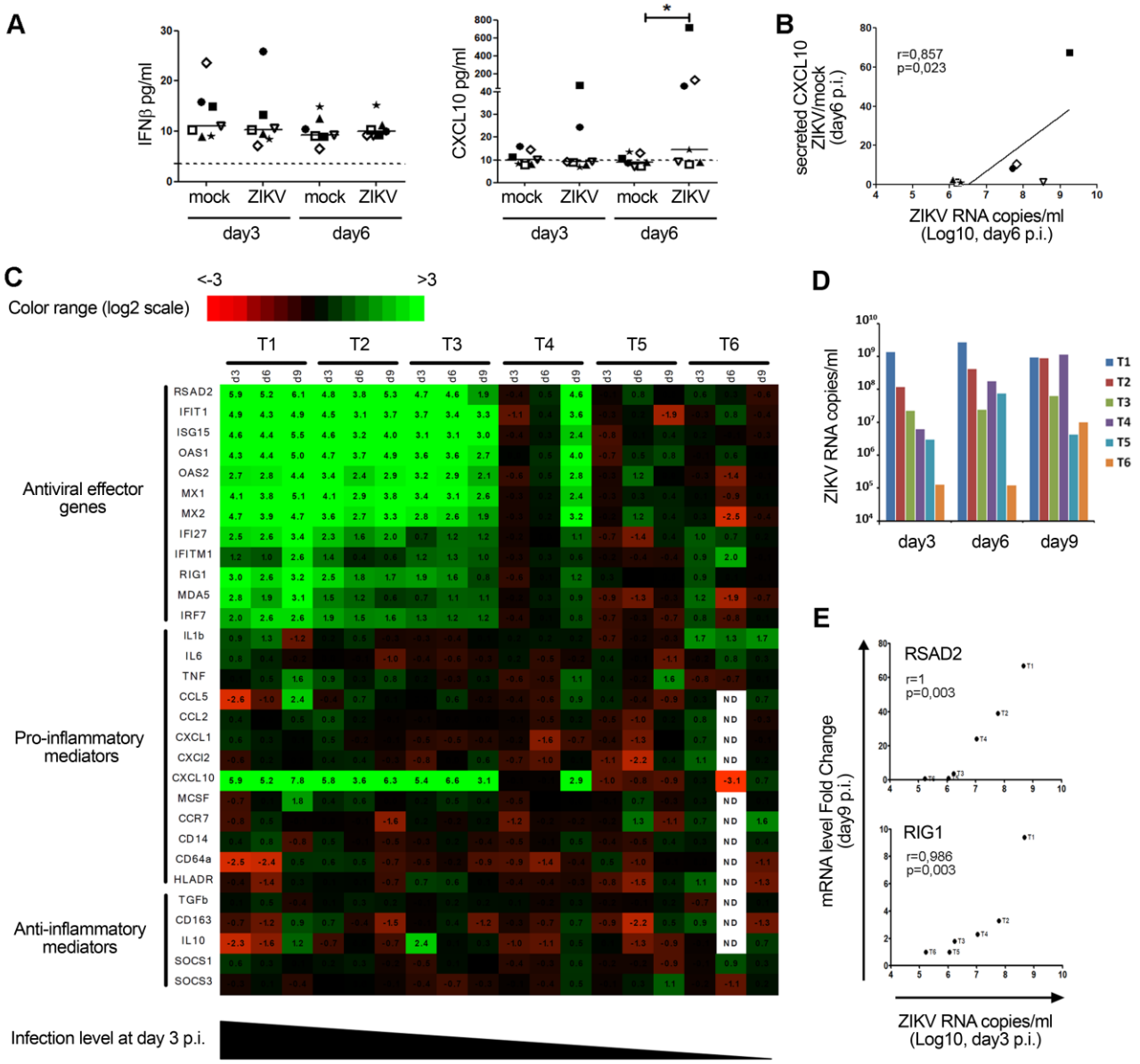

Figure 6 ZIKV triggers a broad antiviral response but no IFN-up-regulation and a minimal pro-inflammatory response in human testicular tissue. A) Levels of IFN-β and CXCL10 measured by flow-cytometer based multiplex assay in mock-infected and ZIKV-infected human testis explant supernatants. Each symbol represents a different donor. Bars represent median values. *P<0,05 (Friedman-Dunns non-parametric comparison). B) Correlation between secreted CXCL10 induction in ZIKV-infected versus mock-infected explants and ZIKV RNA level in culture supernatant at day 6 post-infection (p.i.) (Spearman non-parametric test). C) Innate immune gene expression determined by RT-qPCR in the testis explants from 6 donors (T1-T6) infected with ZIKV for 3, 6 and 9 days (d3, d6, d9). Heat-map shows log2 transformed expression ratios between ZIKV-infected and time-matched mock-infected controls. Green indicates up-regulation and red down-regulation of mRNA compared to controls. Type I and II IFN mRNAs were below the quantification threshold (not shown). D) Viral loads in supernatants of the testis explants analyzed in (C). E) Examples of correlation between gene expression fold at day 9 and the level of infection at day 3 p.i. (Spearman non-parametric test). Other correlations are shown in Figure S9.

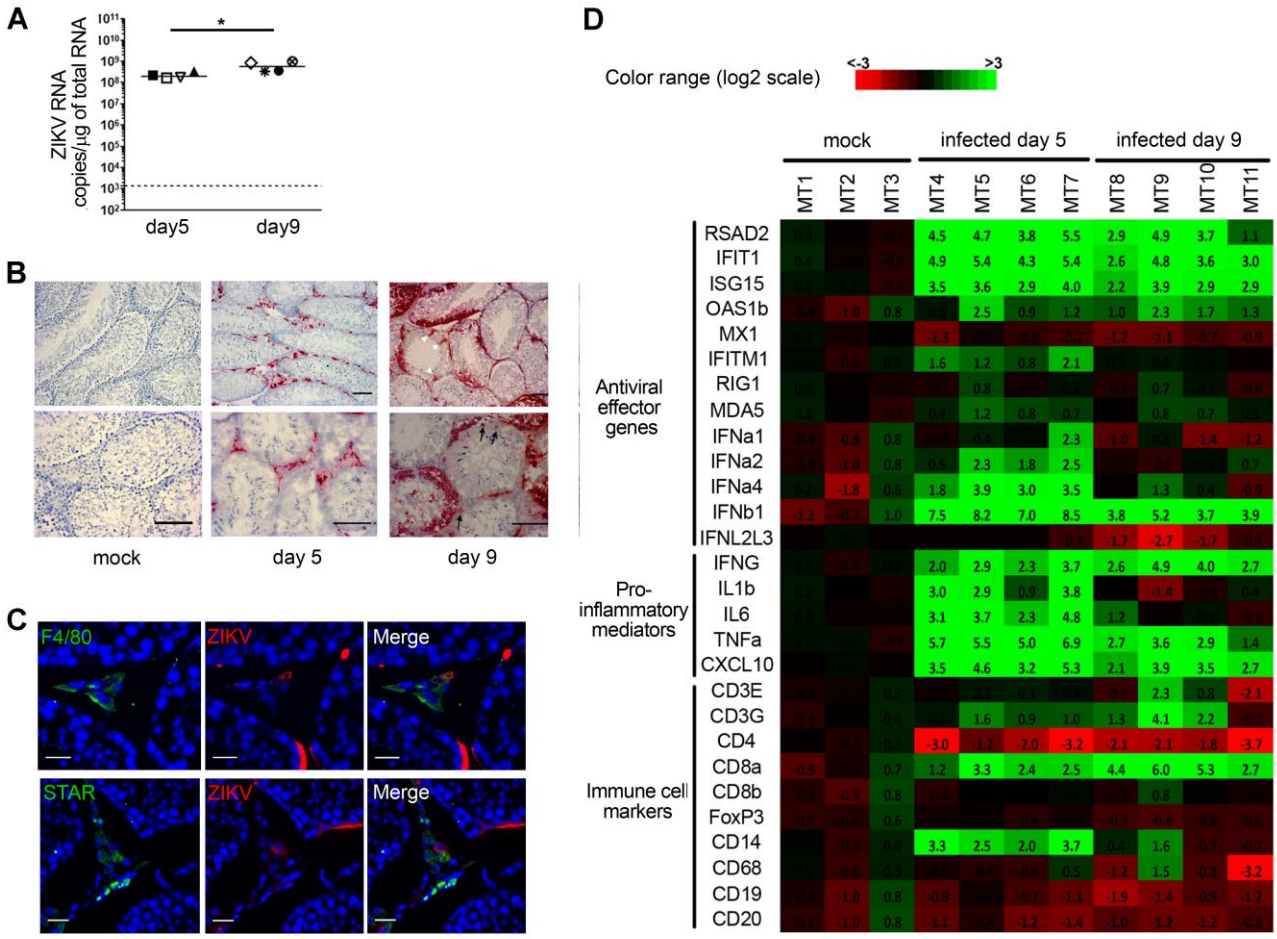

Figure 7 Innate immune response to ZIKV infection in the testis from IFNAR$^{-/-}$ mouse.
A) vRNA measured by RT-qPCR in the testis from mice infected with ZIKV for 5 or 9 days (4 animals/group). Each dot represents one animal and horizontal bars represent the median. The dotted line indicates the limit of detection. Mock-infected (n=3) were below the detection threshold (not shown). * P<0,05 (Mann-Whitney test, non-parametric comparison) . B) Detection of ZIKV RNA by RNAscope in situ hybridization in testis tissue sections from mice mock-infected or at day 5 or day 9 post-infection. White arrow heads point at Sertoli cells, thin black arrows point at germ cells. Scale bars=100um. C) RNAscope in situ hybridization for ZIKV RNA coupled with immunofluorescence for cell markers identified ZIKV RNA in F4/80+ macrophages and STAR+ Leydig cells. Nuclei are stained in blue. Scale bars=20um. D) Expression of a range of innate immune genes and of genes encoding immune cell markers was determined by RT-qPCR in testis from 3 mock-infected mice (mouse testis MT1 to MT3) and 4 ZIKV-infected mice at day 5 (MT5 to MT7) and day 9 (MT8 to MT11) post-infection. Fold induction is presented as a heat-map of log2 transformed expression ratios to the average expression level in mock-infected mice. On the scale bar, green indicates up-regulation and red, down-regulation.